International Journal Of
Industrial Electronics Control and Optimization
Print ISSN: 3517-2645
Online ISSN: 3568-2645
Homepage: https://ieco.usb.ac.ir/

Designing and Fabrication of High Frequency Ultra-wideband Passive Phase Shifters with Single Layer Microstrip Structure and Unequal Source and Load Impedances

Habibollah Zolfkhani [1] | Alireza Sharifi [2]
Department of Electrical Engineering, Faculty of Engineering, University of Zanjan, Zanjan, Iran[1,2]
Corresponding author's email : h.zolfkhani@znu.ac.ir

Article Info

Article type:
Research Article

Article history:
Received: 08-December-2023
Received in revised form: 24-February-2024
Accepted: 02-March-2024
Published online: 21-March-2024

Keywords:
Differential phase shifters Optimization- Computer aided design- Impedance matching, Single layer circuits-Ultra-wideband.

ABSTRACT

In this paper, a method is presented to design and implement ultra-wideband phase shifters, in frequency ranges higher than 10 GHz, with fractional bandwidth near a hundred percent. The phase shifter is constructed from microstrip transmission lines and short circuit stubs. In comparison with conventional phase shifters which are composed of microstrip coupled lines and multilayer structures, the proposed phase shifter has advantages from the implementation and fabrication viewpoint. The design and optimization method is in such a way that arbitrary phase shift, source and load impedances may be considered in the design. To optimize the circuit dimension, a computer code is written, and two design examples are considered. The computer code is based on closed form equations for microstrip transmission lines and available circuit models for it and utilizes microwave network equations. Its results are then improved with electromagnetic full-wave packages to consider the parasitic effects of microstrip T-junctions. Two design cases are included, in the first design, the case of a 45 degrees phase shifter with a standard 50 ohms source and load impedances is investigated. In the second design case, the case of a 90 degrees phase shifter with 50 ohms input impedances and 75 ohm non-standard output impedances is considered. By observing the full-wave simulation results as well as the fabrication and measurement results in these examples, it is clear that the design goals are highly satisfied by this method.

I. Introduction

The technology and engineering revolution seeks to improve the quality of human life and actualize social development. Challenges in social conditions are also extended to physical sciences and engineering. In other words, today's development is intertwined with research related to technology. The answer and solution to the issues and problems for the development of societies lies in electronics and telecommunications. Rarely is there a situation in electronics and telecommunications where the concept of phase changes is not discussed. Basically, in many cases, the main information is in the phase that needs to be extracted. In measurement systems, comparing the phase of signals helps improve the accuracy, quality and reliability of data. Many processes are performed on the phase in the diagnosis and imaging. In engineering, the phase of the reflection coefficient is very useful in detecting the type and geometry of objects by the reflection of electromagnetic waves. Among other applications of phase shifters, it is possible to refer to the cases of power combiners and power dividers, amplifiers, mixers, and radars, especially phased array radars. The ideal phase shifter is an adapted two-port network or

Copyright © *Zolfkhani*, et al.
Publisher: University of Sistan and Baluchestan

circuit without losses, which can change the phase of a specific signal at the desired working frequency with respect to its reference state. Of course, none of the phase shifters are without loss in practice. But it is expected that the losses be low and constant. Phase shifters are divided into, analog or digital, made of integrated or discrete circuit, two-dimensional or three-dimensional circuits and integrated or discrete. working frequency of phase shifters are radio, microwave and millimeter waves. various design and construction methods are presented according to frequency, bandwidth, compatibility with technology, cost, commercial quality and optimality criteria [1-3].

Phase shifters have many applications in communication systems like in any ultra- wideband array antennas with beam steering abilities and ultra-wideband radars with abilities to track transmitters in ultra -wideband frequency ranges. In digital systems, the speed of information transfer is very important. High speed in these systems is equivalent to wide bandwidth in analog systems. Therefore, ultra-wideband phase shifters are one of the main components of great importance. In the structure of the mixer, from the combination of signal RF and LO, signal IF is obtained, with the performance of the mixer depending on the phase shifters RF and LO in the frequency band.

Ultra-wideband (UWB) phase shifters and impedance transformers are key elements in transmitter, receiver communication circuits and array antennas. Phase shifters have been used in multi-beam antennas [4] and multi-channel amplifiers [5]. In differential phase shifters, the signal phase delay passing a main path is compared with corresponding one passing from another path called reference path. An electronically controllable active phase shifter is designed and implemented in Ku band [6]. Passive phase shifters are more stable and have lower costs than active counterparts. So far many designs have been presented to implement differential passive wide-band phase shifters. The most famous one was introduced by Schiffman in 1958 [7], in which he utilized strip line coupled transmission lines in implementing wideband phase shifters. In [8], microstrip coupled line transmission lines are used to obtain Schiffman phase shifter and study the effects of differences between the phase velocities of even and odd modes of the microstrip coupled lines, on the specification of Schiffman phase shifter, This study showed that due to the differences between even and odd mode propagation constant in microstrip coupled transmission lines, the usage of microstrip coupled transmission lines instead of coupled striplines in Schiffman phase shifter will definitely affect its performance. The usage of multi section coupled transmission lines increase the bandwidth of directional couplers and Schiffman phase shifters and with this technique wideband 90 and 180 degree phase shifters are implemented [9]. In [10] asymmetric coupled lines are employed to increases the amount of coupling and bandwidth of coupled-line couplers. In that design, one of the components of coupled line structure is interdigital transmission line and the other is conventional microstrip transmission line.

The common problem with all of the above mentioned works is that for increasing the level of edge coupling in wideband applications, it is required that the distance between the coupled lines be very small, or very narrow transmission lines be used in implementing interdigital transmission lines, which may lead to fabrication difficulties, and the etching tolerances practically limits the operation of these designs to frequencies below 10 GHz.

Other structures are invented that do not utilize microstrip coupled lines to realize phase shifters. In [11], multi-layer structure is used to realize UWB phase shifter in the frequency range 1.3-5.9 GHz. In this design, the above layer is coupled to the bottom one through a slot made in the ground plane between them. This design may have fewer applications in monolithic microwave integrated circuit (MMIC) designs which usually are designed as single layer prototypes. In [12], another UWB phase shifter is designed by means of microstrip to slot line coupling structure in the frequency range 3.1-10.6 GHz and with phase shift in the range 4-27 degrees. No design is introduced out of this phase shift range in that work. The slot lines are made by removing metallic surface from ground plane partially, so it is needed to apply the etching process on both the surfaces above and below the substrate. Also due to the presence of defected ground, that design has radiation loss especially at higher frequencies. In another article [13], microstrip transmission lines and half wavelength open circuited stubs are used to achieve a wideband phase shifter. The phase shift amount was $90^{\circ} \pm 6.4^{\circ}$. The advantages of the design include elimination of coupled lines and remaining of the ground plan unaltered. But the design bandwidth is not enough for covering UWB applications and the high lengths of half wavelength open stubs, result in a larger circuit size. The T-shaped open circuited stub is used to decrease the circuit size in that work. In [14], two multi-sectional radial transmission lines are used instead of T-shaped open circuited stub to increase the bandwidth. The phase shift amount was $90^{\circ} \pm 9^{\circ}$. However these designs have dealt with realizing just 90 degrees phase shifters and seemingly they failed to design circuits that consider the phase shifts below 90 degrees.

On the other hand, wideband impedance matching is inevitable in communication circuits, since the input and output impedances of transmitters, receivers and phase shifters may not necessarily be the standard 50 ohms values. As far as the authors know, all of the works done so far on phase shifters,

are based on standard 50 ohms source and load impedances. For example, none of the studies can apply to a case with the load impedance of 75 ohms. Extra UWB matching circuit is needed after designing the phase shifter, and this will lead to a complicated design process and increased circuit size. The points related to the integration using the theory of transmission lines have been attended in studies [15-17]. Also to the best of author knowledge, the works done on phase shifters so far, support frequencies up to 10.6 GHz, and at higher frequencies no design has yet been presented.

In the current research, a method is illustrated to design and implement the UWB differential phase shifter in the frequency range 6-18 GHz. The proposed method does not use any coupling structure and the ground plane also is not altered. The proposed structure is in single layer type and the design method can satisfy different design goals like arbitrary phase shift values as well as arbitrary source and load impedance levels. The suggested structure uses a simple combination of microstrip transmission lines along with short circuited quarter wavelength stubs. In the part II, below some explanations are given about the theoretical analysis and the phase shifter structure used in this work. Two design cases are presented in parts III and IV the fabrication and simulation results are depicted which further describes the design process.

II. THEORETICAL ANALYSIS

This section shows that combination of two microstrip transmission lines and a quarter wavelength short circuited stub, presents similar phase behavior with Schiffman phase shifter which is constructed from couple striplines [7]. Consider the structure of figure 1. This figure illustrates the base building block of the proposed phase shifter, which has a main path and a reference path. In this figure the characteristic impedances of all transmission lines are assumed to be 50 ohms and the electrical length of all transmission lines in the main path is θ. The input and output impedances of all ports are 50 ohms.

When cascading two-port networks, the overall ABCD matrix is equal to the product of the individual ACBD matrix. in Figure 1, the network consists of three two ports. First, a transmission line, second, a short-circuit parallel transmission line, and third, a transmission line. Their transfer matrix is as follows:

$[ABCD1] = \begin{bmatrix} cos\theta & iz_o sin\theta \\ iy_0 sin\theta & cos\theta \end{bmatrix}$, [ABCD2]=$\begin{bmatrix} 1 & 0 \\ y & 1 \end{bmatrix}$,

[ABCD3]= $\begin{bmatrix} cos\theta & iz_o sin\theta \\ iy_0 sin\theta & cos\theta \end{bmatrix}$

The admittance of the parallel short circuit branch is $y = -iy_o \frac{cos\theta}{sin\theta}$ The product of these three matrices is obtained as

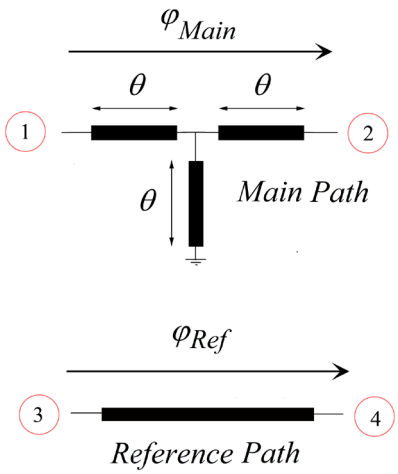


Figure 1- Main and reference paths in the building block of the proposed phase shifter.

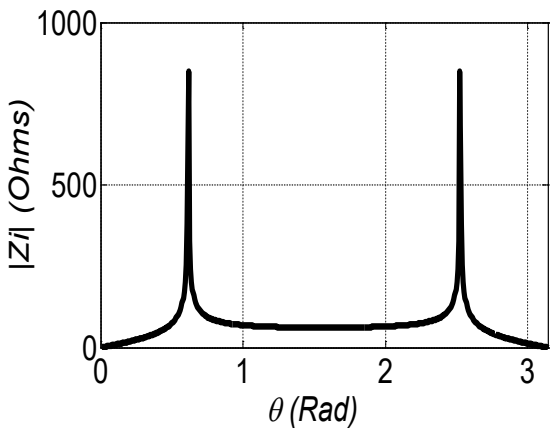


Figure 2- Magnitude of image impedance for the main path in figure 1.

$$[ABCDT] = \begin{bmatrix} A & B \\ C & D \end{bmatrix} = [ABCD1][ABCD2][ABCD1]$$

$$= \begin{bmatrix} 2-3sin^2(\theta) & i75\,sin(2\theta) \\ i\dfrac{2cos(\theta)-3cos^3(\theta)}{50\,sin(\theta)} & 2-3sin^2(\theta) \end{bmatrix} \quad (1)$$

Considering symmetry in figure 1, we have A=D in (1) and the image impedance is obtained from,

$$Z_{i1} = \sqrt{\frac{AB}{CD}} = \sqrt{\frac{B}{C}} = \sqrt{\frac{7500\,sin^2(\theta)}{3sin^2(\theta)-1}} \quad (2)$$

where A, B, C and D are the elements of transmission matrix in figure 1 and are obtained in (1). Magnitude of image impedance is plotted in figure (2). As it can be seen, it is approximately constant equal to 50 ohms in a relatively large bandwidth.

The amount of attenuation α and phase delay ϕ_{Main}, in the main path from port 1 to 2, can be found from $= \alpha + j\beta$.

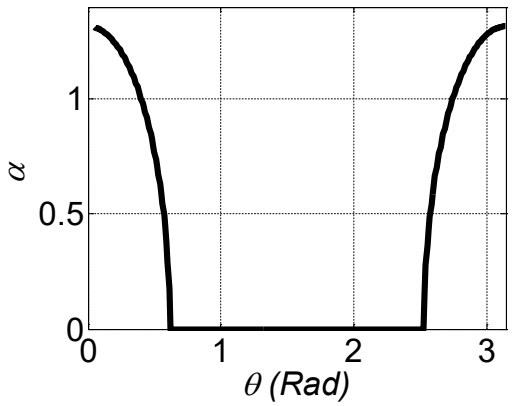


Figure 3- Attenuation amount of the main path in figure 1, obtained by image theory.

where γ is the complex propagation coefficient, α is the attenuation coefficient and β is the propagation constant. The relationship between γ and the elements of transmission matrix, using image theory [18], is as follows,

$$\cosh\gamma = \sqrt{AD} \qquad (3)$$

In figure 3, main path attenuation is provided. Frequency ranges in which $\alpha = 0$, correspond to pass band and the others in which $\alpha \neq 0$, resemble stop band regions. Figure 4, presents the phase delay in the main path ϕ_{Main} and reference path ϕ_{Ref}. Considering that in figure 1, a single transmission line is used in the reference path, which its physical length is proportional to the physical length of one of the transmission lines composing the main path, the electrical length of the reference path ϕ_{Ref} would be proportional with θ, so ϕ_{Ref} versus θ would be a linear function. In figure 4, the ratio ϕ_{Ref} to θ is adjusted in such a way that $\phi_{Ref} - \phi_{Main}$ becomes constant in a relatively wide frequency range. It is concluded that in this figure, ϕ_{Ref} / θ is a little greater than 2.

Comparing the phase difference behavior of the structure in figure 1 and Schiffman phase shifter [7] seems interesting. In figure 5, the Schiffman phase shifter is shown. As is stated in section 1, Stripline coupled transmission lines are used in Schiffman phase shifter. ϕ_{Main} is obtained from [7],

$$\cos(\varphi_{Main}) = \frac{\frac{Z_{0e}}{Z_{0o}} - \tan^2(\theta)}{\frac{Z_{0e}}{Z_{0o}} + \tan^2(\theta)} \qquad (4)$$

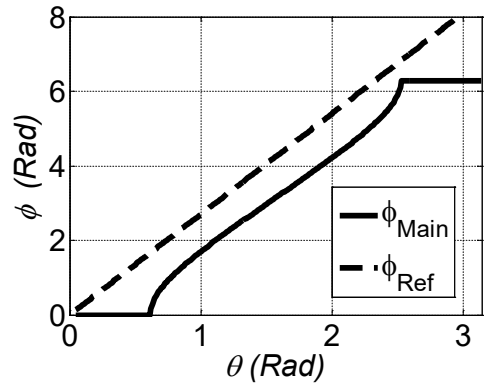


Figure 4- Phase delays in the main path ϕ_{Main} and in the reference path ϕ_{Ref} in figure 1.

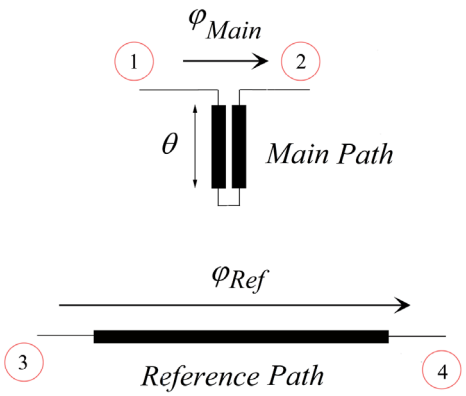


Figure 5 - The structure of differential Schiffman phase shifter

Z_{0o} is odd mode impedance is defined as characteristic impedance of a transmission line with driven signals of the same amplitude and opposite polarity and Z0e is even mode impedance with same amplitude and polarity. ρ is the ratio of these two impedances.

For the case with $\rho = \frac{Z_{0e}}{Z_{0o}} = 10$, which corresponds to tight coupling, and the edge coupled transmission lines must be very close to each other, ϕ_{Main} and ϕ_{Ref} are sketched in figure 6. The length of the reference path is adjusted in such a way that the phase difference $\phi_{Ref} - \phi_{Main}$ becomes nearly constant in a broad bandwidth. In this case, the ratio ϕ_{Ref} / θ becomes approximately 6. Comparing figures 4 and 6, it is apparent that, the bandwidth of figure 1 is better than that of figure 5, and for keeping $\phi_{Ref} - \phi_{Main}$ constant $\phi_{Ref} - \phi_{Main}$ in a wide frequency range, the required length of the reference path in figure 1 can be half the length of the reference path in figure 5, resulting in a reduced dimension for the reference path.

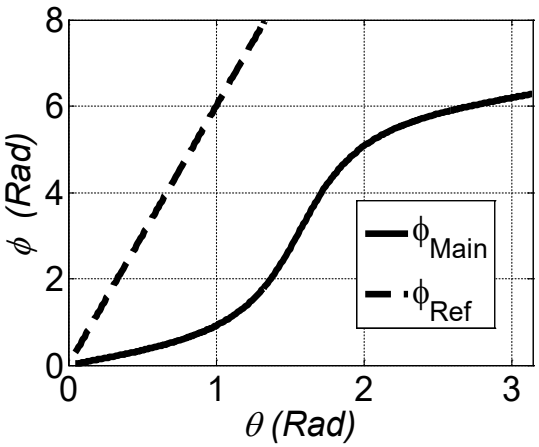


Figure 6 - Phase delays in the main path, ϕ_{Main} and in the reference pat , ϕ_{Ref} , in figure 5.

The problem with the phase shifter structure introduced in figure 1, is that its bandwidth is not still enough to cover UWB applications. Also, this structure is used in a very special case where the impedance of all transmission lines and ports are assumed to be equal to 50 ohms. Also, the electrical length of all transmission lines in the main path are considered equal. In succeeding parts of this paper, extra sections to the configuration of figure 1 are added and the reference path is altered. Moreover, the electrical length and characteristic impedances of composing transmission line of this structure are adjusted. Then, the possibilities of improving the bandwidth of this structure, realizing arbitrary phase shifts and input/output impedances are investigated. In the first example, the case of standard 50 ohms input/output impedance is considered while the phase shift is assumed to be 45 degrees. In the second example, the case of 90 degrees phase shift is presented along with nonstandard 75 ohms output impedances.

III- First Design Example: Phase Shifter with 50 Ohms Input/Output Impedances and 45 Degrees Phase Shift

Figure 7 shows the geometric structure of the proposed phase shifter. In this design the input/output port impedances are assumed to be standard 50 ohms, and 45 degrees phase shift in 6-18 GHz is desired. The reflection coefficient from input ports of the main and reference paths must be as low as possible. In this work, RT-Duroid 5880 substrate with dielectric constant 2.22 and 15 mil thickness is used to realize microstrip transmission lines.

This structure is a multi-section version of the structure in figure 1 to increase its bandwidth, and the reference path

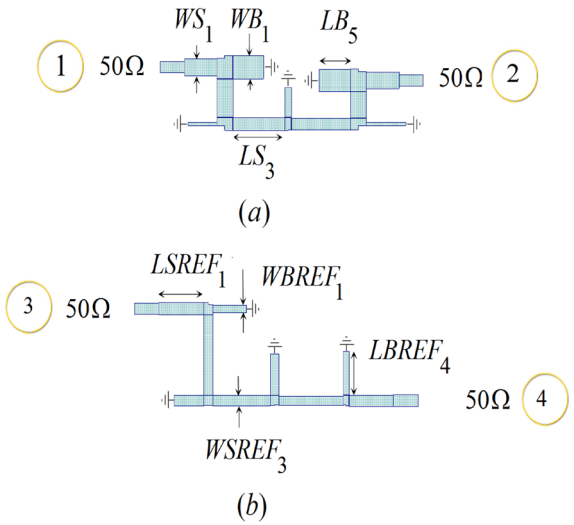


Figure 7- Geometric structure of the proposed phase shifter in the first design example, (a) main path ,(b) reference path.

structure is also considered similar to the reference path one. The number of sections in the main path is 5 and for the reference path is 4. The lengths and widths of all transmission lines are considered as variables in the optimization process. The lengths and widths of transmission lines that are connected in series in the main path are named as LS_i and WS_i, respectively and the ones that belong to the reference path are similarly named as $LSREF_j$ and $WSREF_j$, also The lengths and widths of short circuited stubs that are used in the main path are indicated by LB_i and WB_i and those of the reference path are illustrated by $LBREF_j$ and $WBREF_j$. In figure7, dimensions of some of the exemplary transmission lines are depicted. For ease of fabrication and connecting 50 ohms SMA connectors to the circuit, 50 ohms microstrip transmission lines with length 3 mm and width 1.175 mm are connected to each port. To optimize the dimensions of figure 7, a computer code is written using MATLAB [19]. The following error function is considered,

$$Error = 2\sum_{n=1}^{40}\left[20\,log\left|\bar{S}Main_{11,n}\right| + 30\right]^2 + \sum_{n=1}^{40}\left[20\,log\left|\bar{S}REF_{11,n}\right| + 30\right]^2 + \sum_{n=1}^{40}\left[\left(\angle\bar{S}Main_{21,n} - \angle\bar{S}REF_{21,n}\right) - 45^\circ\right]^2 \quad (5)$$

In (5) it is aimed that the normalized reflection coefficients for the main path and reference path, i.e., $\bar{S}Main_{11,n}$ and

$\bar{S}REF_{11,n}$ become as low as -30 dB. Phase difference between the main path and reference path, i.e., $\left(\angle\bar{S}Main_{21,n} - \angle\bar{S}REF_{21,n}\right)$ must become 45 degrees. Frequency range 6-18 GHz is assumed to be divided into 40 equidistance discrete points. In this special example the emphasis is on reducing the reflection coefficient of the main path rather than the reference path, so the weighting factor in the first term is assigned twice the second term in (5) and section numbers of the reference path is selected less than the main path. In general, assigning weighting factors are somehow experimental and depends on special application.

The normalized scattering matrix coefficients $\left[\bar{S}\right]$ used in (5), can be calculated from non-normalized $[S]$ from,

$$\begin{bmatrix} \bar{S}_{11} & \bar{S}_{12} \\ \bar{S}_{21} & \bar{S}_{22} \end{bmatrix} = \begin{bmatrix} S_{11} & \frac{\sqrt{Z_2}}{\sqrt{Z_1}} S_{12} \\ \frac{\sqrt{Z_1}}{\sqrt{Z_2}} S_{21} & S_{22} \end{bmatrix} \quad (6)$$

Non-normalized scattering matrix for each of the networks in reference and main paths, i.e., $[SREF]$ and $[SMain]$, may be obtained from their transmission matrix, i.e., $\begin{bmatrix} A & B \\ C & D \end{bmatrix}_{REF}$ and $\begin{bmatrix} A & B \\ C & D \end{bmatrix}_{Main}$. Neglecting parasitic effects of T-junctions in initial design step, transmission matrix for the main path can be obtained from multiplication of transmission matrixes of the composing elements of the network, i.e., series transmission lines and short circuit stubs, as

$$\begin{bmatrix} A & B \\ C & D \end{bmatrix}_{Main,f} = \left(\prod_{i=1}^{5} [TS_{i,f}][TB_{i,f}]\right)[TS_{6,f}] \quad (7)$$

Where $\left[TS_{i,f}\right]$ is transmission matrix of the i'th series transmission line at frequency 'f ', and is gotten from [12],

$$[TS_{i,f}] = \begin{bmatrix} \cosh\gamma S_{i,f} LS_i & ZS_{i,f} \sinh\gamma S_{i,f} LS_i \\ \frac{1}{ZS_{i,f}} \sinh\gamma S_{i,f} LS_i & \cosh\gamma S_{i,f} LS_i \end{bmatrix} \quad (8)$$

Where $\gamma S_{i,f} = \alpha S_{i,f} + j\beta S_{i,f}$ is the propagation constant , $ZS_{i,f}$ and LS_i are the characteristic impedance at frequency *'f'*, and physical length of i'th series transmission line . $\gamma S_{i,f}$ and $ZS_{i,f}$ are functions of transmission line dimensions and substrate specifications. In the computer program, closed form equations for microstrip transmission lines which are valid to 60 GHz and consider all frequency dispersion and attenuation effects [18]. In (9), $\left[TB_{i,f}\right]$ is the transmission matrix for the i'th short circuited stub at frequency *'f'* and is obtained from,

$$\left[TB_{i,f}\right] = \begin{bmatrix} 1 & 0 \\ \frac{1}{ZB_{i,f} \tanh\gamma B_{i,f} LB_i} & 1 \end{bmatrix} \quad (9)$$

Where $\gamma B_{i,f} = \alpha B_{i,f} + j\beta B_{i,f}$ is the propagation constant and $ZB_{i,f}$ and LB_i are the characteristic impedance at frequency *'f'*, and physical length of i'th short circuited stub.

Normalized scattering matrix for the reference path may be calculated through the same method as applied in the above for the main path. This network is considered as a 4 section one, so its transmission matrix is obtained as,

$$\begin{bmatrix} A & B \\ C & D \end{bmatrix}_{REF,f} = \left(\prod_{i=1}^{4} [TSREF_{i,f}][TBREF_{i,f}]\right)[TSREF_{5,f}] \quad (10)$$

Where in this equation, similar to (8), (9)

$$[TSREF_{i,f}] = \begin{bmatrix} \cosh\gamma SREF_{i,f} LSREF_i & ZSREF_{i,f} \sinh\gamma SREF_{i,f} LSREF_i \\ \frac{1}{ZSREF_{i,f}} \sinh\gamma SREF_{i,f} LSREF_i & \cosh\gamma SREF_{i,f} LSREF_i \end{bmatrix} \quad (11)$$

$$\left[TBREF_{i,f}\right] = \begin{bmatrix} 1 & 0 \\ \frac{1}{ZBREF_{i,f} \tanh\gamma BREF_{i,f} LBREF_i} & 1 \end{bmatrix} \quad (12)$$

Where $\gamma SREF_{i,f} = \alpha SREF_{i,f} + j\beta SREF_{i,f}$ is the propagation constant , $ZSREF_{i,f}$ and $LSREF_i$ are the characteristic impedance at frequency *'f'*, and physical length of the i'th series transmission line in the reference path and $\gamma BREF_{i,f} = \alpha BREF_{i,f} + j\beta BREF_{i,f}$ is the propagation constant , $ZBREF_{i,f}$ and $LBREF_i$ are the characteristic impedance at frequency *'f'*, and physical length of the i'th short circuited stub in the reference path.

After obtaining the elements of scattering matrix for the networks in the main path and reference path from the above relations, the error function in (5) must be minimized. To start the optimization, initial values must be considered for all variables. In the first design example, since input/output impedances are assumed to be 50 ohms, in order to apply

impedance matching conditions at center frequency, the initial physical lengths for all transmission lines located in the main path, are assumed to be a quarter wavelength at center frequency, i.e., 12 GHz, and initial characteristic impedances of all transmission lines in the main and reference paths are considered equal to 50 ohms. In order to set $\left(\angle\bar{S}Main_{21} - \angle\bar{S}REF_{21}\right)$ equal to 45° at center frequency, total physical length of the reference path is considered longer than main path in which the length difference becomes equivalent to - 45 degrees phase shift at the center frequency. Then the length of all transmission lines in the reference path are assumed the same. Optimization is done with the following flowchart.

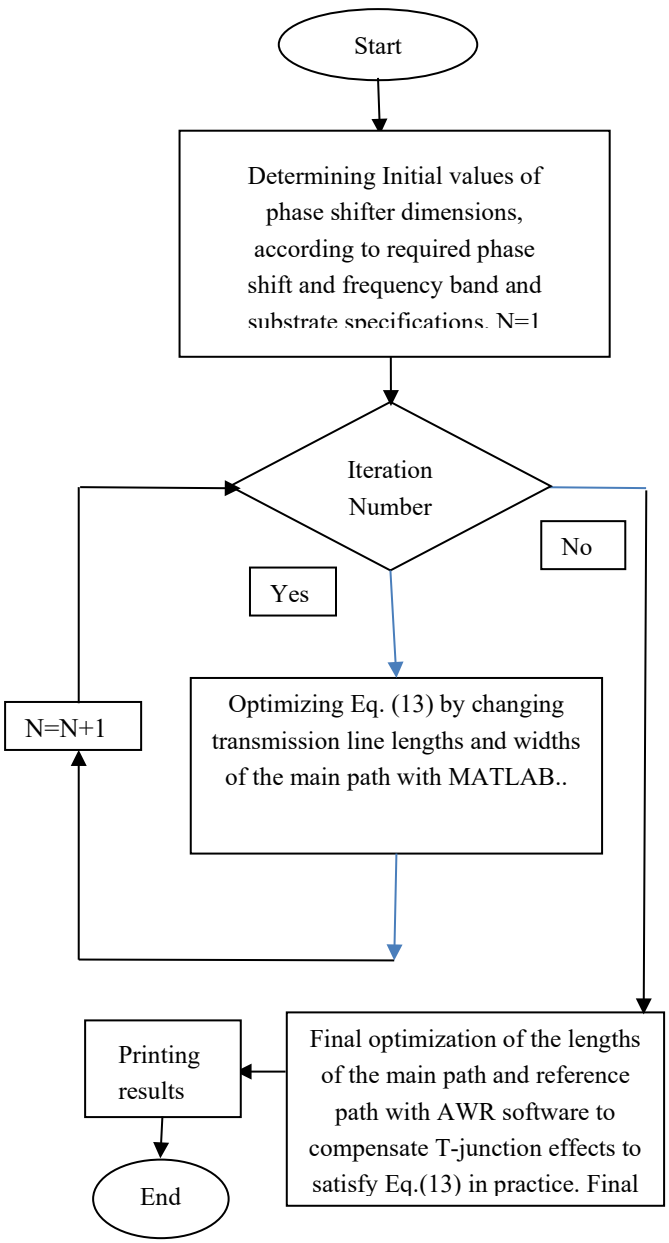


Table 1- dimensions of the designed phase shifter in the first design example obtained by computer program and fine tuning by EM softwares.

	*	**		*	**
WS_1	1.81	1.81	LS_1	4.27	4.18
WS_2	1.99	1.99	LS_2	4.35	3.4
WS_3	1.36	1.36	LS_3	5.98	7.24
WS_4	1.28	1.28	LS_4	6.03	7.23
WS_5	1.95	1.95	LS_5	3.73	2.61
WS_6	1.81	1.81	LS_6	4.25	3.8
WB_1	2.42	2.42	LB_1	4.09	3.75
WB_2	0.38	0.38	LB_2	3.31	3.64
WB_3	0.83	0.83	LB_3	3.26	2.95
WB_4	0.38	0.38	LB_4	4.10	4.93
WB_5	2.38	2.38	LB_5	4.14	3.95
$WSREF_1$	1.27	1.27	$LSREF_1$	4.43	5.49
$WSREF_2$	1.13	1.11	$LSREF_2$	7.62	8.34
$WSREF_3$	1.08	1.06	$LSREF_3$	7.45	7.01
$WSREF_4$	1.13	0.94	$LSREF_4$	7.66	7.82
$WSREF_5$	1.35	1.14	$LSREF_5$	3.87	5.39
$WBREF_1$	0.53	0.8	$LBREF_1$	3.99	4.12
$WBREF_2$	1.15	1.08	$LBREF_2$	3.69	3.65
$WBREF_3$	1.16	1.07	$LBREF_3$	3.77	4.32
$WBREF_4$	0.66	0.69	$LBREF_4$	3.88	4.56

* Circuit dimensions obtained by computer program (mm)
** Circuit dimensions after fine tuning with EM softwares

While optimization is running, some limitations are imposed on the transmission line lengths and widths, in such a way that the designed structure be practically implementable. This strategy, also prevents creation of T-junctions with large parasitic effects. The computer program is run on a core(TM) i3 system with CPU clock 2.13 GHz and after 5600 (s) (less than 2 hours), gives the results. The initial error function value is decreased from initial value 58458 to final value 5128. The circuit dimensions which are obtained by the program, are mentioned in table 1. The designed structure is then analyzed by AWR [20] and HFSS [21] full-wave EM softwares. To partially compensate the parasitic effects of T-junctions, assuming that main path transmission line widths be constant, physical lengths of transmission lines are fine tuned. The final dimensions are outlined in table 1.The simulated structure in HFSS software is shown in figure 8. This design is fabricated which its photograph is presented in figure 9. The scattering matrix of this design is measured using Agilent 8722ES Network Analyzer and the measurement results are compared with outcomes of full-wave simulations and computer program.

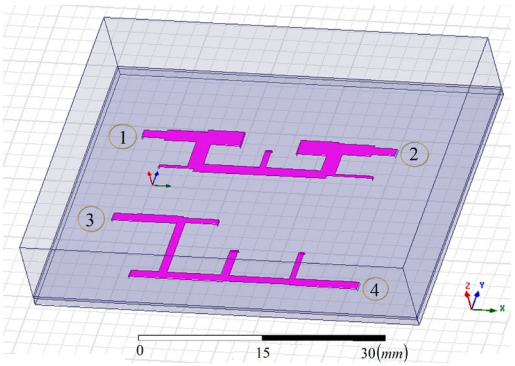


Figure 8- simulated structure for the first design example in HFSS software.

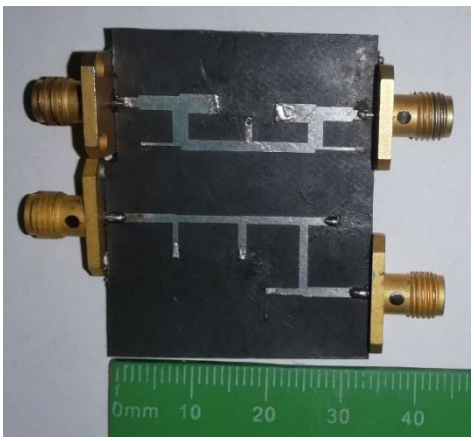


Figure 9- Photograph of the fabricated structure for the first design example.

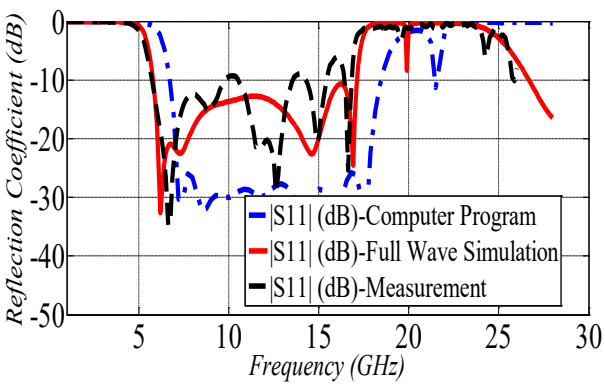


Figure 10- Computer program, full-wave simulation and measurement results for reflection coefficient of the main path.

Figures 10 to 13 are plots of computer program results, full-wave simulations and measurements for transmission and reflection coefficient for the main and reference paths respectively.

Figure 14 shows the comparing results of the computer program, full-wave simulation and measurement for the phase difference between the main and reference paths.

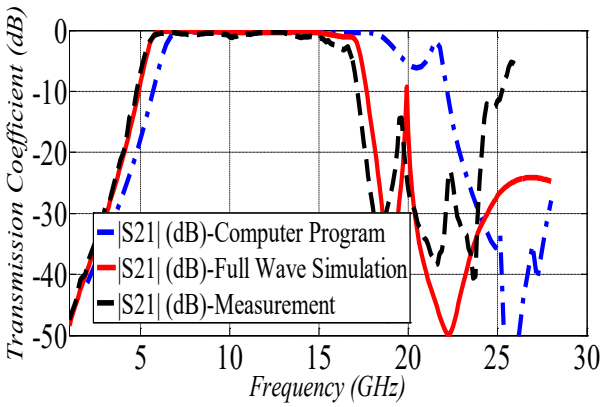


Figure 11- Computer program, full-wave simulation and measurement results for transmission coefficient of the main path.

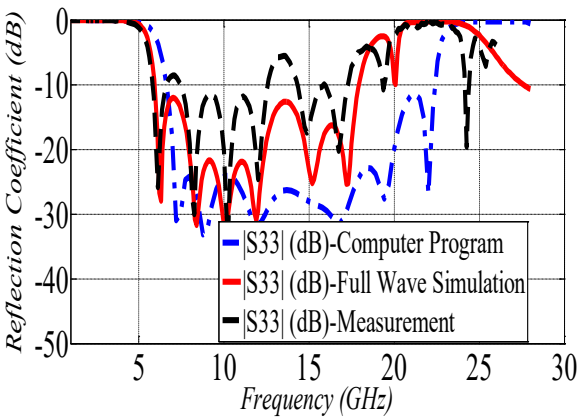


Figure 12- Computer program, full-wave simulation and measurement results for reflection coefficient of the reference path.

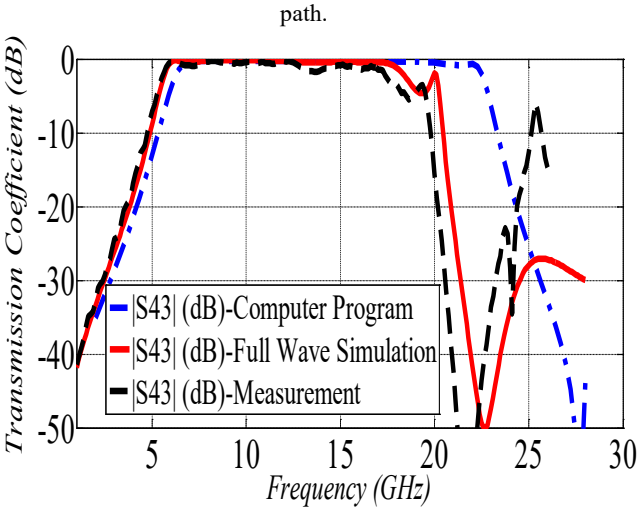


Figure 13- Computer program, full-wave simulation and measurement results for transmission coefficient of the reference path.

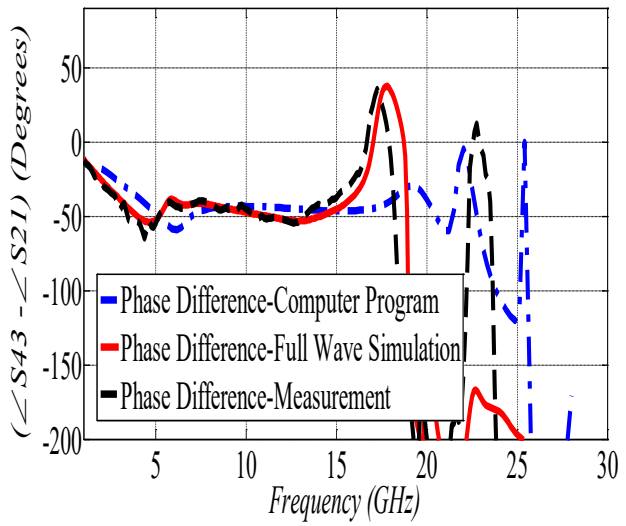


Figure -14 - Comparing results of the computer program, full-wave simulation and measurement for the phase difference between the main and reference paths.

In this design example, full wave simulation results for the main and reference paths reflection coefficient are better than -10 dB in the frequency range 6-18 GHz. The obtained full wave simulation phase shift in frequency band 5-17 GHz is $-45^{\circ} \pm 8^{\circ}$. Differences between full-wave simulation and circuit model analysis are due to the presence of parasitic effects in which are not completely modeled in the computer program and couldn't be exactly fine tune by EM software. Measurement results are in good correspondence with simulation results and minor discrepancies may arise from fabrication tolerances, connector losses, non-ideal short circuits, measurement errors, etc. As is stated in (5), in this special example, the emphasis on reducing the main path reflection coefficient is considered twice that of the reference path. In applications which the reflection coefficient of the reference path must be reduced in the same way as the main path, equal weighting factors must be considered in the error function and more sections may be included in the reference path.

IV- SECOND DESIGN EXAMPLE

In this example, we show the ability of the proposed method in considering nonstandard input/output impedances in designing phase shifters. In this example, it is assumed that impedances of input ports 1 and 3 be 50 ohms and the impedances of output ports 2 and 4 be 75 ohms. The phase difference between main and reference paths is aimed to be -90 degrees in the range 6-18 GHz. The main path and reference path structure of this example is seen in figures 15(a) and (b), respectively. Structures of the main path in the first and second

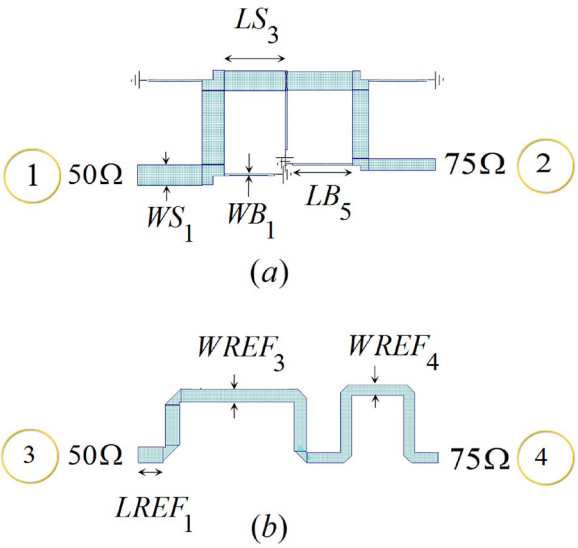


Figure 15- (a) and (b) show main and reference paths in the second phase shifter design example, respectively.

design example is similar and have 5 sections, but in current example, in the reference path, a 4 section impedance transformer is used. Dimensions of some exemplary transmission lines are illustrated in figure 15.

The following error function is employed to optimize circuit dimensions in this example,

$$Error = 4\sum_{n=1}^{40}\left[20\,log\left|\bar{S}Main_{11,n}\right| + 30\right]^2 + \sum_{n=1}^{40}\left[20\,log\left|\bar{S}REF_{11,n}\right| + 30\right]^2 + \sum_{n=1}^{40}\left[\left(\angle\bar{S}Main_{21,n} - \angle\bar{S}REF_{21,n}\right) - 90^{\circ}\right]^2 \quad (13)$$

Considering (13), the weighting factor of reflection coefficient reduction in the main path is considered 4 times more than the reference path. In here to start optimization, initial values are needed too. In the main path, the characteristic impedances of all transmission lines in short circuited stubs are assumed to be 50 ohms, and their electrical length is considered quarter a wavelength at the center frequency. These stubs so, are seen as open circuit at their inputs in the center frequency and would have no impact on input signal. Then to match input and output port impedances, the impedance of all series transmission lines are set equally as $\sqrt{ZL1 \times ZL2}$ and their electrical lengths are also selected equal to quarter a wavelength at center frequency. The main path is composed of 6 series transmission lines, so the phase delay from port 1 to 2 would be $-6 \times 90^{\circ} = -540^{\circ}$, at center frequency. The reference path, is realized using 4 series transmission lines. The initial characteristic impedances of all these lines are chosen equal to $\sqrt{ZL1 \times ZL2}$. In this

Table 2- Circuit dimensions of the designed phase shifter in the second example after optimization with computer program and fine tuning with EM softwares.

	*	**		*	*
WS_1	1.4	1.4	LS_1	4.40	4.40
WS_2	1.52	1.52	LS_2	5.03	5.03
WS_3	1.36	1.36	LS_3	4.19	4.19
WS_4	1.27	1.27	LS_4	4.45	4.45
WS_5	1.09	1.09	LS_5	4.67	4.67
WS_6	0.81	0.81	LS_6	4.54	4.54
WB_1	0.15	0.15	LB_1	4.48	3.40
WB_2	0.12	0.12	LB_2	4.46	3.71
WB_3	0.12	0.12	LB_3	4.84	4.03
WB_4	0.11	0.11	LB_4	4.68	3.99
WB_5	0.11	0.11	LB_5	4.63	4.11
$WREF_1$	1.10	1.10	$LREF_1$	4.49	1.69
$WREF_2$	0.97	0.97	$LREF_2$	4.60	2.80
$WREF_3$	0.85	0.85	$LREF_3$	18.29	11.89
$WREF_4$	0.73	0.73	$LREF_4$	4.62	18.20

* Circuit dimensions obtained by computer program (mm)
** Circuit dimensions after fine tuning with EM softwares (mm)

example, the relation $\left(\angle\bar{S}Main_{21,n} - \angle\bar{S}REF_{21,n}\right) = 90^\circ$ must be satisfied. So it is necessary that total phase delay in the reference path from port 1 to 2, becomes $-7\times 90^\circ = -630^\circ$, at center frequency. So initial lengths of all transmission lines in the reference path are set equally with $630^\circ / 4 = 157.5^\circ$. The computer program after running on the same computer system in previous design example, gives results after 1094 seconds; less than an hour. The initial error function is 5711224 and the final one is 364. The circuit dimensions after optimization with computer program are listed in table 2. The designed circuit is then simulated with full wave methods and to compensate parasitic effects of T-junctions and microstrip bends, dimensions of the structure is adjusted, in which corrections can be seen in table 2. Final dimensions are very close to the results of computer program and solely some of the transmission line lengths are altered. Figure16 presents the simulated structure in HFSS software.

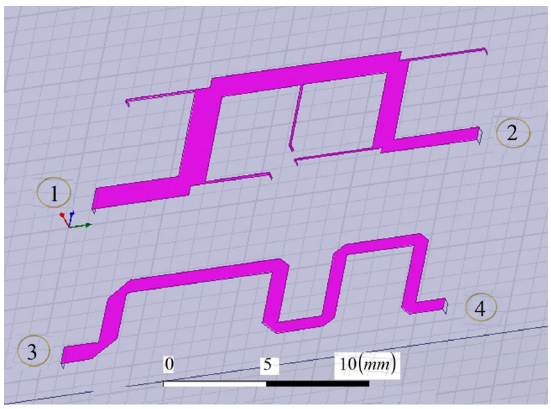


Figure 16- Simulated structure in HFSS software for the second design example.

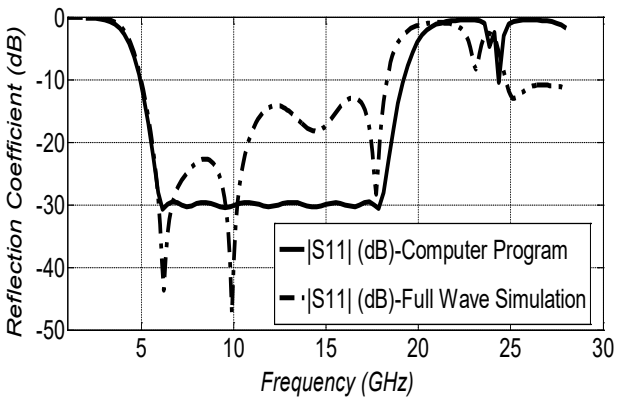


Figure 17- Computer program and full-wave simulation results of the reflection coefficient for the main path in the second design example.

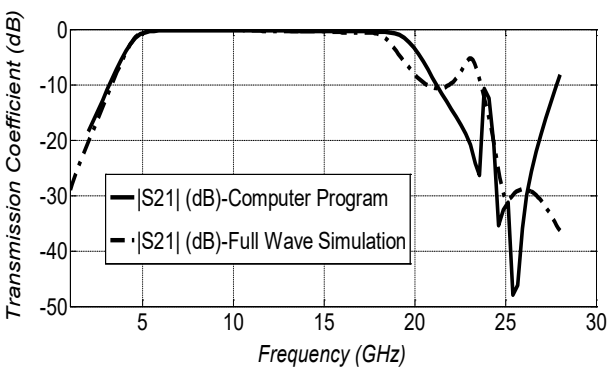


Figure 18- Computer program and full-wave simulation results of transmission coefficient for the main path in the second design example.

Computer program and full-wave simulation results of the reflection and transmission coefficients for the main and reference paths are respectively illustrated by figures 17,18,19,20. Figure 21 compares the phase difference among the main and reference paths obtained by computer program and HFSS simulations.

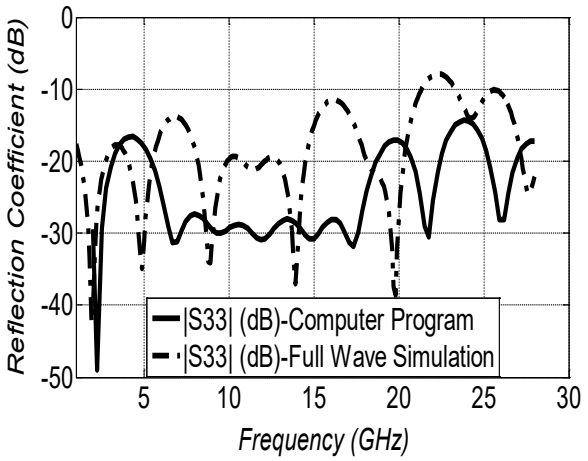


Figure 19- Computer program and full-wave simulation results of the reflection coefficients for the reference path in the second design example.

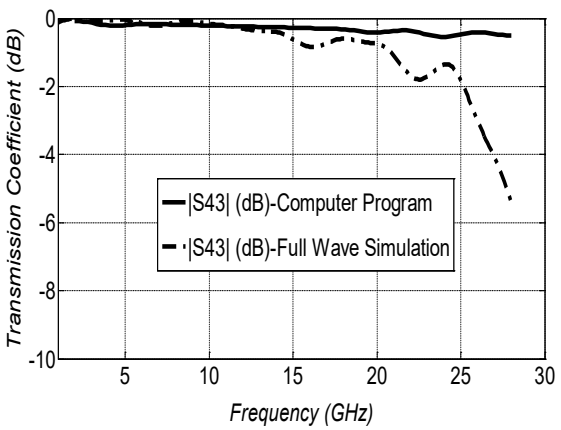


Figure 20- Computer program and full-wave simulation results of the transmission coefficient for reference path in the second design example.

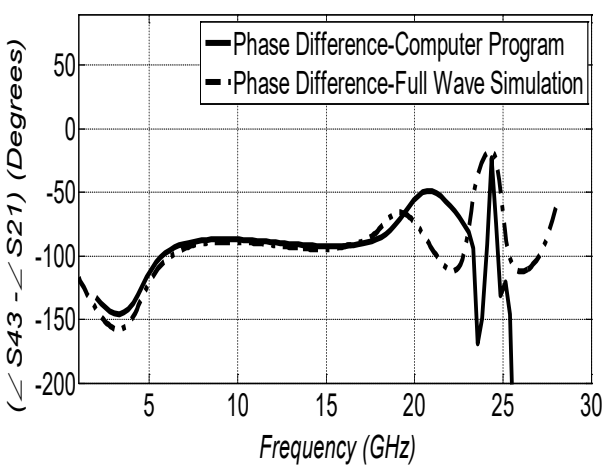


Figure 21- Computer program and full-wave simulation results of the phase difference between main and reference paths in the second design example.

In this example, full wave simulation of the reflection coefficient for the main and reference paths better than -10 dB in 6-18 GHz are acquired and the phase shift $-90^{\circ} \pm 8^{\circ}$ is obtained in 6.5-17.7 GHz. The designed circuit as well as creating almost constant phase shift with fractional bandwidth near to a hundred percent, successfully matches input 50 ohm source impedance to output 75 ohm load impedance. From the above figures it is clear that computer program results are very close to full wave simulations for the final fine tune structure. It is deduced that the written computer program works correctly and the existing differences between the results arise from parasitic effects that are ignored to be modeled completely in the written code. Any other phase shifters with phase shift values other than the above mentioned examples and with arbitrary source and load impedances in arbitrary frequency ranges may be designed by the written computer program in a relatively fast time.

V- CONCLUSION

In this paper, two UWB phase shifters with applications in 6-18 GHz were investigated. To realize these phase shifters, combinations of microstrip transmission lines and short circuit stubs were used in multi-section mode to provide required bandwidth. At the first design step, a computer program based on optimizing an error function was written, using exact closed form equations for microstrip transmission lines. To avoid complexity in the program, parasitic effects of T-junctions were ignored. After this initial design, which is relatively fast and exact, to overcome the parasitic effects of T-junctions, final fine tuning was done on the lengths of transmission lines using full wave simulations. To illustrate the proposed design method, two different design examples were depicted. In the first design, input/output impedances were 50 ohms and desired phase shift difference was assumed to be -45 degrees. In the second design, a more general structure with unequal source and load impedances were considered in the case of -90 degrees phase shift difference. In both designs, acceptable results were obtained from the full wave simulation and measurements which satisfy design goals for transmission and reflection coefficients and phase shift differences in the design bandwidth

REFERENCES

[1] Arati Arun Bhonkar, Dr. Udaysinh Sutar, “Overview of Microstrip Line Phase Shifter,” international Journal of Advanced Research in Computer and Communication Engineering, Vol. 5, Issue 5, pp. 465-469, May 2016.

[2] Jialong Zeng , Yuxin Ren , Cheng Tan , Yang Yuan , Jiaxuan Li and Zhongjun Yu, “ An 8–18 GHz 90◦ Switched T-Type Phase Shifter,” micromachines , pp.1-10, 7 August. 2023

[3] Ferran martin and Francico medina, “Balanced Microwave

Transmission Lines Circuits, and Sensors," IEEE journal of Microwaves , Vol. 3, Issue 1. pp. 398-440, 6 january 2023.
[4] Krzysztof Wincza, Slawomir Gruszczynski, "Broadband Integrated 8 × 8 Butler Matrix Utilizing Quadrature Couplers and Schiffman Phase Shifters for Multibeam Antennas With Broadside Beam," IEEE TRANSACTIONS ON MICROWAVE THEORY AND TECHNIQUES, Vol. 64 , No. 8 , pp. 2596 – 2604, Aug. 2016.
[5] A. Angelucci, P. Audagnotto, P. Corda, and B. Piovano, Multiport, "power amplifiers for mobile-radio systems using microstrip Butler matrices, " in Int. Symp. Antennas Propag. (AP-S), Dig., Vol. 1, pp. 628–631,1994.
[6] Padilla P, Muñoz-Acevedo A, Sierra-Castañer M., "Low loss 360° Ku band electronically -reconfigurable phase shifter," AEU–Int J Electron Commun, Vol. 64, Issue 11, pp. 1100-1104, 2010.
[7] B. Schiffman, "A new class of broadband microwave 90-degree phase shifters," IRE Trans. Microw. Theory Tech., Vol. MTT-6, No. 4, pp. 232–237, Apr. 1958.
[8] C. Free and C. Aitchison, "Improved analysis and design of coupled line phase shifters," IEEE Trans. Microw. Theory Tech., Vol. 43, No. 9, pp. 2126–2131, Sep. 1995.
[9] B. Schiek and J. Kohler, "A method for broadband matching of microstrip differential phase shifters," IEEE Trans. Microw. Theory Tech., Vol. MTT-25, No. 8, pp. 666–671, Aug. 1977.
[10] Keshavarz R, Movahhedi M, Abdipour A," A broadband and compact asymmetrical backward coupled-line coupler with high coupling level," AEU–Int J Electron Commu, Vol. 66, Issue 7, pp. 569-574, 2012.
[11] Somayeh Khajepour, Shahrooz Asadi, Mohammad Saeid Ghaffarian, Gholamreza Moradi, "Design of Novel Wideband Reflective Phase Shifters with Wide Range of Phase Applications," AEU–Int J Electron Commun, Vol. 71, pp. 30-36, 2017.
[12] M. N. Moghadasi, G. Dadashzadeh, A. Dadgarpour, F. Jolani, B. S. Virdee, " COMPACT ULTRA-WIDEBAND PHASE SHIFTER", Progress In Electromagnetics Research Letters, Vol. 15, pp. 89-98, 2010
[13] Zheng SY, Chan WS, Man KF," Broadband phase shifter using loaded transmission line", IEEE Microw. Wireless Compon. Lett. Vol. 20, Issue 9, pp.498–500. 2010.
[14] Yeung SH, Mei Z, Sarkar TK, Salazar-Palma M , " Design and testing of a single-layer microstrip ultra-wideband 90 differential phase shifter", IEEE Microw. Wireless Compon. Lett. Vol. 2013, Issue 23, pp. 122-124, 2013.
[15] J. Zhou, H. J. Qian and X. Luo, "Compact Wideband Phase Shifter Using Microstrip Self-Coupled Line and Broadside-Coupled Microstrip/CPW for Multiphase Feed-Network," in IEEE Microwave and Wireless Components Letters, Vol. 27, No. 9, pp. 791- 793, Sept. 2017.
[16] H. Zhu and A. M. Abbosh, "A Compact TunableDirectional Coupler with Continuously Tuned Differential Phase," in IEEE Microwave and Wireless Components Letters, Vol. 28, No. 1, pp. 19-21, Jan. 2018.
[17] Denis A.Letavin , "Compact Two-Position Phase Shifter, " Telfor Journal , Vol.14 , No.1, pp. 39-43, 2022.
[18] Pozar, D.M. (1998). Microwave Engineering (2nd edition). John Wiley.
[19] Math Work In ," Optimization Toolbox of MATLAB 7.4.0.287 (R2007a) Software", January 2007.
[20] Applied Wave Research, Inc. (2006). AWR Design Environment (Version 7.03).
[21] Ansoft Corporation (2007). Ansoft HFSS (Version 11).



Habibollah Zolfkhani was born the city of Zanja 1963. He received the B.S degree in electrical engineering form university of Tehran in 1988 and 1991 respectively .From 1991 to 2000, he worked as lecturer mostly in the field of education and education development at Zanjan of University From. 2000 to 2005, he completed his doctoral and postgraduate studies and received his PhD from Iran University of Science and Technology. Since then, he has been working as an assistant professor at University of Zanjan. His educational and research fields focus on applied electromagnetics, MEMS and the analysis and design of RF and Microwave circuits.



Alireza Sharifi was born in Malayer Iran,in 1979. He received the B.Sc. degree in electrical Engineering from Shahid Beheshti University Tehran, Iran, in 2001, the M.Sc. degree in Electrical engineering from the Iran University of Science and Technology (IUST), Tehran, Iran, in 2004, and the Ph.D. degree in electrical engineering at IUST, Tehran, Iran, in 2011. He is currently an assistant professor at the University of Zanjan, Zanjan, Iran. His research interests are in various areas of electrical engineering such as high-frequency circuit design and the application of numerical methods in electromagnetics, antennas, microwave circuits, and photonics. He has completed several projects on electronic and communication circuits